Structural Resolution of the Initiation of Actomyosin's Force Generating Stroke

Yang Zhenhui

for the Degree of Doctor of Philosophy

Supervisor: András Málnási-Csizmadia PhD.

Structural Biochemistry Doctoral Program,

Doctoral School in Biology

Program Leader: Prof. László Gráf DSc.

Head of the School: Prof. Anna Erdei DSc.

Eötvös Loránd University
Budapest, Hungary
2012

Introduction

Different isoforms of myosin play crucial roles in muscle contraction and series of other biological functions. In order to fulfill such various tasks, the effective work of the myosin lever movement, the ATPase cycle, the actin binding and detachment cycle must be harmonized. In ATP-bound and actin detached form of myosin, lever is moved from the so called "down" position to the "up" position (called recovery step); while after ATP hydrolysis, actin rebinds to the "up" lever state of myosin and the lever moves to the "down" position (called power stroke). The actin binding cleft of myosin is a spacious surface, divided by a deep cleft. The strength of actin binding is regulated by the movement of this cleft, as myosin binds to actin weakly in the open- and strongly in the closed-cleft states.

In this thesis, we present *in silico* simulations of the recovery step and structural modeling of actomyosin in the weak actin-binding state, which state is experimentally difficult to approach because of its low proportions in the enzymatic cycle. One of the major questions was whether actin binding induces structural rearrangements in myosin or not. We modeled both the weak and the strong actin-binding states applying protein-protein docking and relaxed it by molecular dynamic simulations. We revealed a novel actin-binding site in myosin named activation loop. The conserved positively charged tip (Arg520) of the activation loop interacts with four negatively charged residues in the N-terminus of actin in both the weak and the strong actin-binding states. Three specific myosin conformational changes induced by actin binding were observed in the weak actin-binding state. The R520Q mutation in the myosin activation loop prevented these conformational changes. It raised the question that what the communication pathways are in the myosin between the actin binding regions and the active sites in the weak actin-binding state? Two communicational pathways were speculated between the actin binding regions and the myosin nucleotide binding site, which might explain the actin-induced myosin conformational changes at the initial stage of the power stroke.

We were also interested in whether the power stroke of myosin runs in the same conformational reaction coordinates as the reverse of the recovery step. Thus, we simulated the conformational pathway of the recovery step. Our results show a three-phase model of the recovery step based on the free energy profile. We also found that the post-recovery state in a lower free energy is more preferred than the pre-recovery state. Formation of hydrogen bond

cluster accelerates structural transformation to overcome the activation energy barrier in the first phase. I present a flow chart based on the main carried out procedures and analyses in Figure 1.

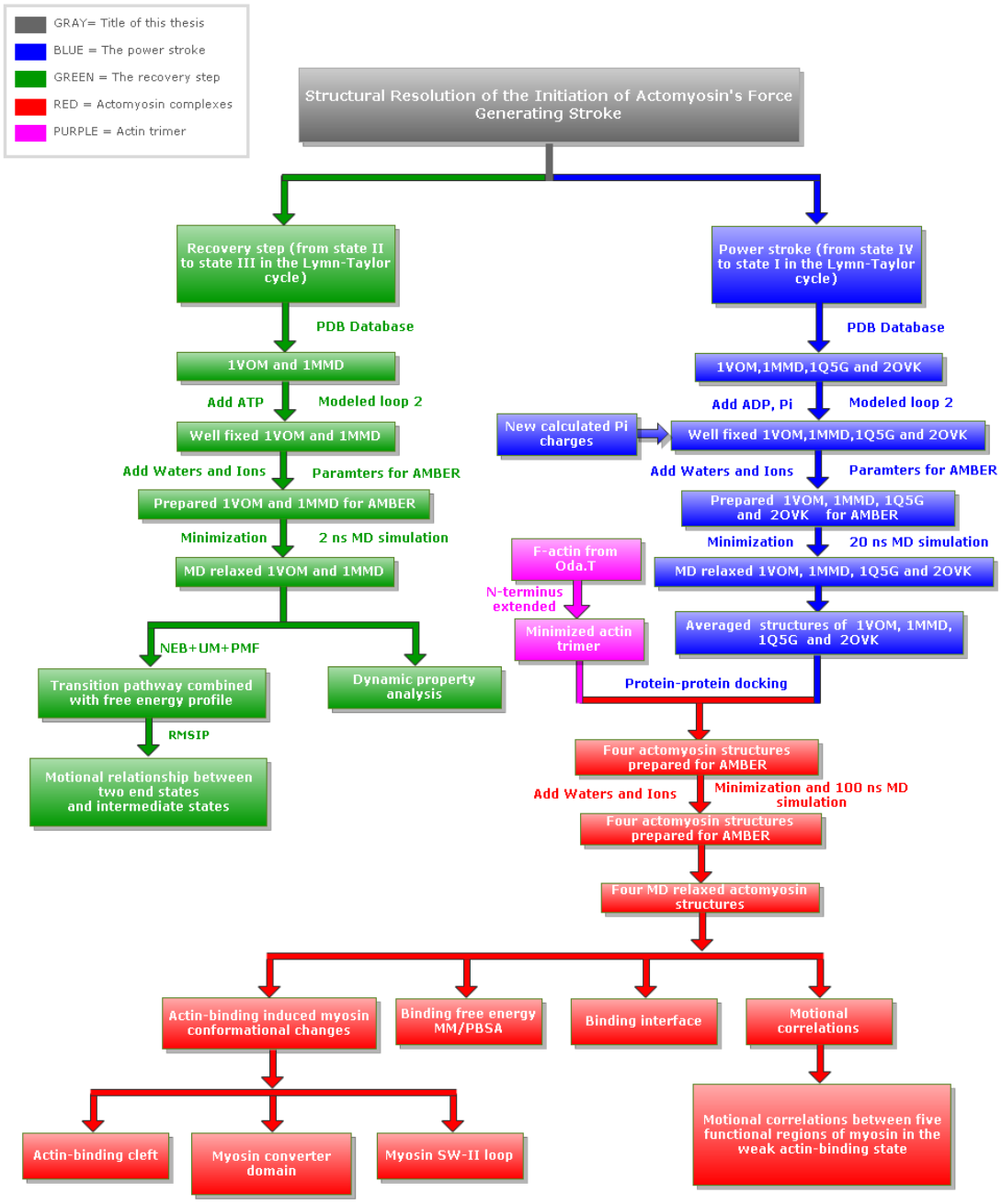

Figure 1: Flow chart of the corresponding procedures regarding to this thesis.

Aims and questions

After ATP hydrolysis in the absence of actin, the rate limiting up-to-down lever swing step (reverse recovery step) occurs. In this case, the lever swing is inefficient regarding the

mechanical cycle since the swing happened in the actin detached state of myosin. If actin weakly binds to the up lever state of myosin, the rate of lever swing step is highly accelerated. The actin activation of the lever swing step channels the reaction pathway into the effective power stroke which mechanism is called kinetic pathway selection. It is interesting to know whether the power stroke of myosin runs in the same conformational reaction coordinates as the reverse of the recovery step. The following questions were stated upon the design of the project:

(1) Although a direct structural trajectory of the recovery step has been deduced from previous *in silico* simulations, it neglected the dynamic behaviors of the protein that allows it to populate the neighboring conformational spaces along the suggested trajectory. Therefore, the question is how can we combine the intermediate states with the suggested structural trajectory to discover the complete mechanism of the down-to-up lever swing of the recovery step?

(2) The precise mechanism of the up-to-down lever swing of the power stroke is still unclear due to limited structural information on the weak actin-binding state. What is the atomic structure of the weak actomyosin complex?

(3) What conformational changes are induced by actin binding in the different states of myosin?

(4) What are the differences of the binding interfaces of both the weak and the strong actomyosin complexes?

(5) The effective pathways of the power stroke are not accessible due to the short lifetime of their intermediates. What is the structural pathway and the possible mechanism of the actin-binding induced myosin up-to-down lever swing in the power stroke?

Applied methods

1. Crystal structures of myosin II (1VOM, 1MMD, 1Q5G and 2OVK) were retrieved from the protein databank. The original ADP analogues as substrates in the myosin nucleotide-binding pocket were converted to Mg·ATP or Mg·ADP·Pi based on the conformational overlapping for both the recovery step and the power stroke, respectively. Charges of protonated phosphate were calculated by Gaussian and ANTECHAMBER programs.
2. The missing loop 2 region of myosin in the structure of 1MMD was rebuilt according to

the coordinate's reconstruction of segment matching by MODELLER and an integrated analytical bioinformatics program (called "Friend").

3. The module of sander in the molecular dynamics package AMBER11 was used for minimization and molecular dynamic (MD) simulations. The final average structure and motional correlations can be revealed according to the MD trajectories.
4. Two averaged *Dictyostelium* myosin II motor domain structures named as $1MMD_{wild}$ (down lever/ATP state/actin detached state) and $1VOM_{wild}$ (up lever/ATP state/actin detached state) after MD simulations were used for exploring the transition pathway of the recovery step according to the nudged elastic band method combined with umbrella sampling. All explored configurations from umbrella sampling were analyzed with the weighted histogram analysis method (WHAM) to determine the potentials of mean force (PMF) for the recovery step.
5. Quantitative characterizations of the dynamical properties of two intermediate states (IM-1 and IM-2) and two end states ($1VOM_{wild}$ and $1MMD_{wild}$) were determined from essential motional analysis by using a covariance matrix in the recovery step based on the means of the root-mean square inner product (RMSIP).
6. Four averaged myosin structures ($1VOM_{md}$, $1MMD_{md}$, $1Q5G_{md}$ (no nucleotide state) and $2OVK_{md}$ (no nucleotide state of molluscan myosin motor domain)) after MD simulations were docked to the refined actin trimer by HADDOCK. Four actomyosin complexes obtained from the protein-protein docking were relaxed in long term MD simulations and named as 3A-$1VOM_{md}$, 3A-$1MMD_{md}$, 3A-$1Q5G_{md}$ and 3A-$2OVK_{md}$. In order to discover the actin-binding effect on the conformational changes of myosin, R520Q, R562Q were introduced to these four actomyosin complexes.
7. In order to distinguish the weak and strong actin-binding states, binding free energy was calculated with the approach of molecular mechanic Poisson-Boltzmann surface area (MM/PBSA). The contribution of entropy based on the ligand receptor association was performed with normal-mode analysis.

Results

1. Two wild type and six mutant motor domain constructs (the mutations were located

around the pivot of the relay/converter/lever swing) in the pre-recovery structure do not show significant differences in their relay-helix regions. However, the conformations of mutants in the post-recovery state show deformation in the kink region of the relay-helix of myosin.

2. In the pre-recovery structure (down lever state), the mobility of the Φ and Ψ angles of the double mutants (F481A/F482A) at the pivoting point is not changed compared to the wild type. However, the averaged amplitudes of the mobility increase more than 50% at the position of (Ψ486/Φ487) and (Ψ488/Φ489) in the double mutants (F481A/F482A). Meanwhile, the averaged amplitudes of the Ψ491/Φ492 in the double mutants (F481A/F482A) drop to 50% compared to the wild type.
3. The free energy of the pre-recovery state (-16.3 kcal·mol^{-1}) is 5.02 kcal·mol^{-1} higher than that of the post-recovery state (up lever state) (-21.32 kcal·mol^{-1}) and the activation free energy of the recovery step is 10.15 kcal·mol^{-1}. Two obvious free energy wells were discovered and named as intermediate state 1 (called IM-1: -17.4 kcal·mol^{-1}) and intermediate state 2 (called IM-2: -15.84 kcal·mol^{-1}). The γ-phosphate~Gly457~Asn475 hydrogen bond cluster began to form in the A' state of Figure 2.
4. Transition from the pre-recovery state to the IM-1 state only accounted for ~37% in the rotation angle of the converter domain of the entire recovery step. The essential motion similarity between the IM-1 state and the post-recovery state is 0.72 similar to the value of 0.69 calculated between the IM-1 state and the pre-recovery state (see Figure 2).
5. The simulated actomyosin binding free energies of 3A-1VOM$_{md}$ and 3A-1MMD$_{md}$ are similar (-7~-8 kcal·mol^{-1}) and higher than those of the 3A-1Q5G$_{md}$ and 3A-2OVK$_{md}$ (-11~-13 kcal·mol^{-1}). These values are parallel with experimental values.
6. In 3A-1VOM$_{md}$, the interaction formed between Arg520 of myosin and Asp1 of actin is also presented in the 3A-1MMD$_{md}$. Arg520, located in the activation loop of myosin, forms strong contacts with residues Asp1 and Asp3/Glu4 of actin in 3A-1Q5G$_{md}$ and 3A-2OVK$_{md}$ (see Figure 3).
7. The partial closure of the actin-binding cleft and the further up rotation of the lever arm induced by the actin binding were observed in the weak actin-binding state (see Table 1). 1VOM$_{md}$ and 3A-1VOM-520MU display similar distances openness in the nucleotide-binding pocket (i.e. switch II loop position) (10.37±0.2Å and 10.21±0.19 Å

respectively). However, noticeable closure were observed in 3A-1VOM$_{md}$ and 3A-1VOM-LP3MU (in which mutation was located in another actin binding site) with the values of 9.44±0.22Å and 9.53±0.18Å.

8. Motinal correlations between the functional regions of myosin were significantly changed by actin binding. We showed that these changes are propagated from actin through the interaction between the activation loop and the actin N-terminal region.
9. In the weak actin-binding state, two communicational pathways were speculated between the actin binding regions and the myosin nucleotide binding site. The first route starts from the activation loop to the SW-II loop through a hydrophobic cluster between the activation loop and the N-terminal of relay-helix. The second route starts from the apex of the helix-loop-helix to the "prestrut" region based on the bonds of Asn588-Asp530/Ser533, and then from the "prestrut" region to the SW-II loop based on the bond of Lys587-Glu467 (see Figure 3).

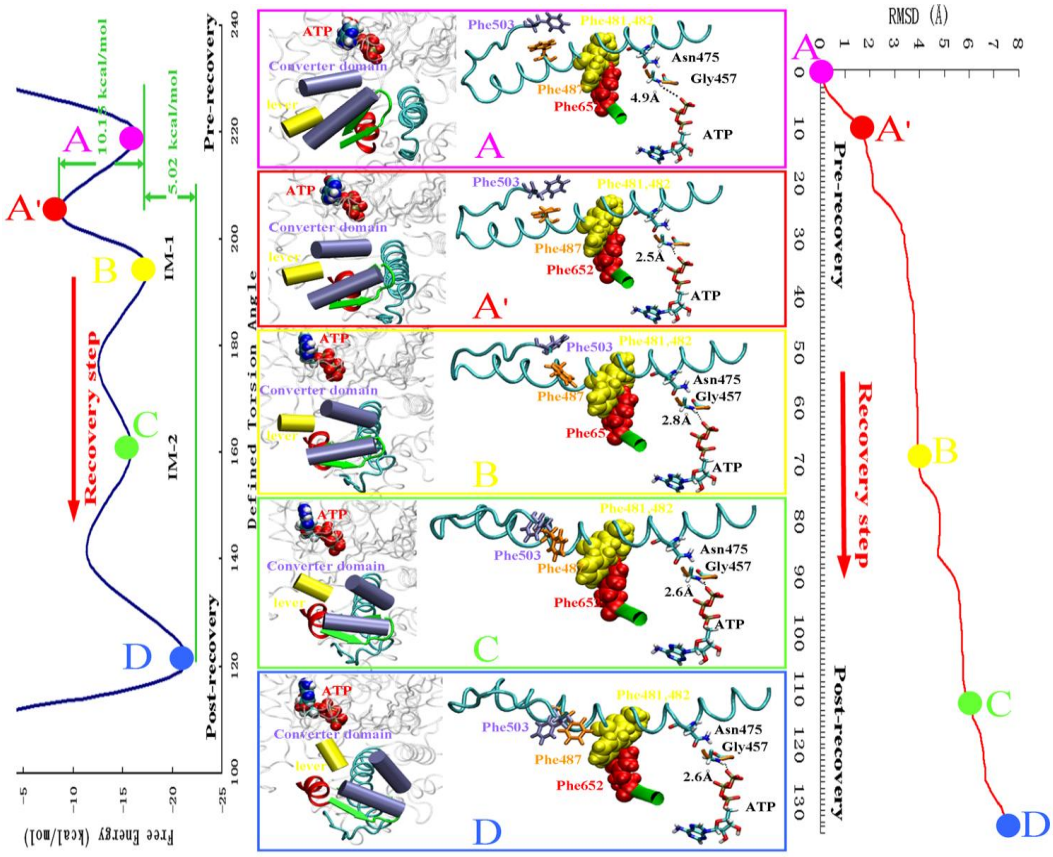

Figure 2: A three phase coupling mechanism is combined with free energy in the recovery step. The left panel shows the free energy profile with two intermediate states and one transition state. The five differently colored points represent the pre-recovery state (A), the transition state (A'), intermediate state-1 (IM-1: B), intermediate state-2 (IM-2: C) and the post-recovery state (D). The points colored in the same way represent the same states based

on the RMSD calculation in the right panel. In the middle panel, conformations of the relay-helix and the converter domain of myosin are boxed with different colors corresponding to the five various states in both the left and the right panel.

Table 1: Angle changes of the converter domain and conformational changes of the actin-binding cleft in different myosin structures

Name	Distance(Å)	Angle(°)	Name	Distance(Å)	Angle(°)
$1VOM_{md}$	21.7	122.73°	$3A\text{-}1VOM_{md}$	20.57	105.03°
$1MMD_{md}$	21.37	203.96°	$3A\text{-}1MMD_{md}$	21.14	227.22°
$1Q5G_{md}$	16.72	220.69°	$3A\text{-}1Q5G_{md}$	11.91	221.73°
$2OVK_{md}$	18.25	220.58°	$3A\text{-}2OVK_{md}$	16.82	245.27°
			Holmes's model	17.23	237.9°
			3A-1VOM-520MU	23.66	120.12°
			3A-1VOM-LP3MU	21.76	111.07°

Angle changes of the converter domain were measured by three residues Gly684 and Arg689 from "SH1 helix" and Ala748 at the end of the converter domain. Angle calculation was based on the CA atom of the three residues with Arg689 in the middle. The conformational changes of the actin-binding cleft were calculated on the basis of the distance between the backbone carbon atom of myosin Glu365 and myosin Asn537.

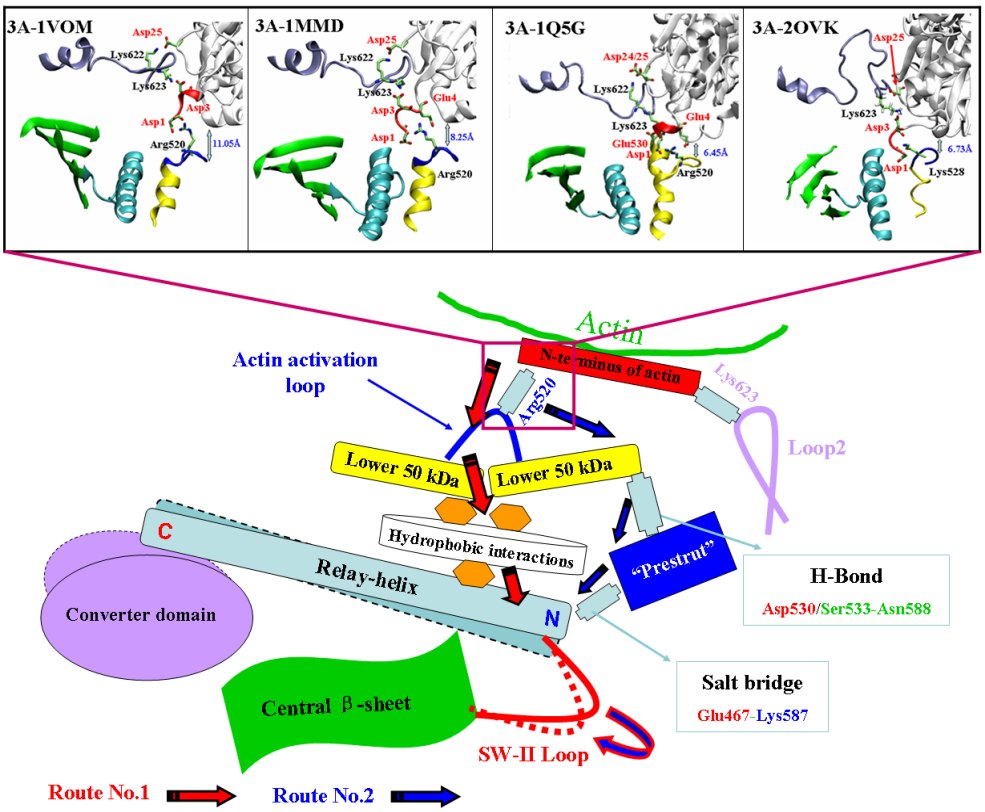

Figure 3: Two efficient routes between activation loop and SW-II loop. In the weak actin-binding state, two communicational pathways were speculated between the actin activation loop and SW-II loop. The four small pictures at the top of this figure represent interactions between the N-terminus of actin and the activation loop in different actomyosin states.

Thesis points:

After the investigation of the recovery step, and the weak binding actomyosin complex as the beginning of the power stroke, we conclude the following:

First: Strain along the relay-helix of myosin is rearranged by eliminating the pivoting point in the seesaw-like motions at the beginning stage of the recovery step.

Second: A three-phase model of the recovery step deduced on the basis of a free energy profile with the post-recovery state in a lower free energy is more preferred than the pre-recovery state.

Third: In the three-phase model of the recovery step, the formation of the hydrogen bond cluster (γ-phosphate~Gly457~Asn475) accelerates structural transformation to overcome the activation energy barrier in the first phase.

Fourth: Intermediate state 1 (IM-1) has similar conformation to the unique intermediate state of Fischer's model, but the IM-1 state with a 37% converter domain rotation is in a middle structural state of the recovery step which was not demonstrated before.

Fifth: The weak and strong actin-binding states of actomyosin were obtained by protein-protein docking and long time-range molecular dynamics relaxations. The lower binding free energy of the strong actin-binding state is due to the involvement of more residues in the binding surface than that of in the weak actin-binding state.

Sixth: The conserved positive tip (Arg520) of the activation loop interacts with four negatively charged residues in the N-terminus of actin in various binding patterns of weak and strong actin-binding state.

Seventh: Three specific myosin conformational changes induced by the actin binding were observed in the weak actin-binding state: 1. the partial closure of the actin-binding cleft, 2. the further up rotation of the lever arm and 3. further closure of SW-II loop. The R520Q mutation in myosin prevented these conformational changes.

Eighth: The motions of the activation loop are correlated with four functional regions of myosin (loop 2, the N-terminus of the relay-helix, the SW-II loop and the "prestrut" region) in the weak actin-binding state which weakens upon actin detachment or by mutational disruption between the activation loop and the N-terminal region of actin.

Ninth: Two communicational pathways were speculated between the actin binding regions

and the myosin nucleotide binding site, which might be a reasonable mechanism of the actin-induced myosin conformational changes at the initial stage of the power stroke.

Conference presentations

Yang Z, Várkuti BH, Málnási-Csizmadia A. 2009. Structural models of the weak binding actomyosin complexes. *38th European muscle conference, Lille.*

Conference abstracts

Yang Z, Várkuti BH, Málnási-Csizmadia A**.** 2011. Molecular dynamic simulation is used for research of the muscle contractions. *Amber 2011 workshop, Barcelona.*

Yang Z, Málnási-Csizmadia A. 2008. Molecular dynamic simulation is used for investigating the mechanism of the seesaw motions in the recovery step. *37th European Muscle Conference, London.*

Publications concerning this thesis

Várkuti BH, **Yang Z,** Kintses B, Erdélyi P, Bárdos-Nagy I, Kovács AL, Hári P, Kellermayer M, Vellai T, Málnási-Csizmadia A. 2012. A novel actin binding site of myosin required for effective muscle contraction. Nat. Struct. Mol. Biol., 19(3):299-306. (Shared first authorships)

Kintses B, **Yang Z,** Málnási-Csizmadia A. 2008. Experimental investigation of the seesaw mechanism of the relay region that moves the myosin lever arm. J. Biol. Chem., 283(49):34121-34128.

Other publications

Simon Z, Peragovics A, Vigh-Smeller M, Csukly G, Tombor L, **Yang Z,** Zahoránszky-Kőhalmi G, Végner L, Jelinek B, Hári P, Hetényi C, Bitter I, Czobor P, Málnási-Csizmadia A. 2012. Drug Effect Prediction by Polypharmacology-Based Interaction Profiling. J. Chem. Inf. Model., 52(1):134-145.